SANDIA REPORT
SAND2006 -7573
Unlimited Release
Printed November, 2006

Development of a Novel Technique to Assess the Vulnerability of Micro-Mechanical System Components to Environmentally Assisted Cracking

David G. Enos and Steven H. Goods

Prepared by
Sandia National Laboratories
Albuquerque, New Mexico 87185 and Livermore, California 94550

Sandia is a multiprogram laboratory operated by Sandia Corporation,
a Lockheed Martin Company, for the United States Department of Energy's
National Nuclear Security Administration under Contract DE-AC04-94AL85000.

Issued by Sandia National Laboratories, operated for the United States Department of Energy by Sandia Corporation.

Available to DOE and DOE contractors from
U.S. Department of Energy
Office of Scientific and Technical Information
P.O. Box 62
Oak Ridge, TN 37831

Telephone: (865) 576-8401
Facsimile: (865) 576-5728
E-Mail: reports@adonis.osti.gov
Online ordering: http://www.osti.gov/bridge

Available to the public from
U.S. Department of Commerce
National Technical Information Service
5285 Port Royal Rd.
Springfield, VA 22161

Telephone: (800) 553-6847
Facsimile: (703) 605-6900
E-Mail: orders@ntis.fedworld.gov
Online order: http://www.ntis.gov/help/ordermethods.asp?loc=7-4-0#online

SAND2006-7573
Unlimited Release
Printed November, 2006

Development of a Novel Technique to Assess the Vulnerability of Micro-Mechanical System Components to Environmentally Assisted Cracking

David G. Enos
Corrosion and Electrochemical Science Department

Steven H. Goods
Analytical Materials Science Department

Sandia National Laboratories
P.O. Box 5800
Albuquerque, NM 87185-0888

Abstract

Microelectromechanical systems (MEMS) will play an important functional role in future DOE weapon and Homeland Security applications. If these emerging technologies are to be applied successfully, it is imperative that the long-term degradation of the materials of construction be understood. Unlike electrical devices, MEMS devices have a mechanical aspect to their function. Some components (e.g., springs) will be subjected to stresses beyond whatever residual stresses exist from fabrication. These stresses, combined with possible abnormal exposure environments (e.g., humidity, contamination), introduce a vulnerability to environmentally assisted cracking (EAC). EAC is manifested as the nucleation and propagation of a stable crack at mechanical loads/stresses far below what would be expected based solely upon the materials mechanical properties. If not addressed, EAC can lead to sudden, catastrophic failure. Considering the materials of construction and the very small feature size, EAC represents a high-risk environmentally induced degradation mode for MEMS devices. Currently, the lack of applicable characterization techniques is preventing the needed vulnerability assessment. The objective of this work is to address this deficiency by developing techniques to detect and quantify EAC in MEMS materials and structures. Such techniques will allow real-time detection of crack initiation and propagation. The information gained will establish the appropriate combinations of environment (defining packaging requirements), local stress levels, and metallurgical factors (composition, grain size and orientation) that must be achieved to prevent EAC.

Table of Contents

Report Format

This report represents the final report for an LDRD project. As such, the report is organized into four discrete sections – an introduction/background/proposed approach (below), followed by three sections detailing the accomplishments for each of the three fiscal years over which the program ran. The conclusions, and recommendations should this work be continued, are presented along with the FY06 accomplishments in the final section.

Section 1 – Introduction, Background, and Proposed Approach

Microelectromechanical systems (MEMS) will play an important functional role in the design and refurbishment of current and future weapon systems, in addition to other critical DOE and Homeland Security applications. If these emerging technologies are to be successfully developed, it is imperative that the long-term behavior of the materials of construction be understood. That is, the scope of this understanding must extend beyond the functioning of the device in the near term – the relevant environmental degradation mechanisms must also be characterized. Unlike electrical devices, MEMS devices have a mechanical aspect to their function – as such, specific components can be subjected to stresses above and beyond whatever residual stresses exist from fabrication. This situation requires that consideration be given to environmentally assisted cracking (EAC). EAC is a form of long-term degradation that can occur in a susceptible structural component given the proper combination of environmental conditions and residual or externally imposed stress state. EAC is poorly understood, very difficult to predict, and if not addressed can lead to sudden, catastrophic failure. In a nutshell, EAC is manifested as the nucleation and propagation of a stable crack at mechanical loads/stresses far below what would be expected based solely upon the materials fracture mechanics (e.g., toughness, sample geometry). It is important to note that the environment does not necessarily have to be very corrosive. The impact of this cracking could range from catastrophic failure of structural components within the device, to improper device function (e.g., changed spring constants, altered tribological properties, etc.). Considering the materials of construction and the very small feature size, EAC represents the highest risk of all possible environmentally induced degradation modes for micro-mechanical devices.

As this LDRD project commenced, there were two primary types of materials being considered by Sandia for manufacturing MEMS devices – single or polycrystalline silicon (SMM) and electrodeposited nickel and nickel alloys (LIGA). The susceptibility of both of these material types in the bulk form to EAC has been well documented in the literature. For example, bulk polysilicon is quite susceptible to sub-critical crack growth in the presence of water vapor. Similarly, wrought nickel-based alloys, particularly those containing elevated sulfur levels (very similar in composition to those developed by Sandia for LIGA based fabrication), are susceptible to both hydrogen embrittlement and intergranular stress corrosion cracking. As such, EAC mechanisms potentially relevant to MEMS materials include hydrogen embrittlement (LIGA), stress-corrosion cracking (LIGA), and sub-critical crack growth (SMM). Unfortunately, the wealth of

existing data for the bulk form of these materials cannot be used to conclusively predict the performance of MEMS devices because the mechanical properties of our MEMS materials are, in general, very different than the bulk analogues. Thus, our existing knowledge base can really only be used to predict potential susceptibility, rather than define the actual EAC behavior of MEMS materials.

Previous work on understanding the mechanical properties of MEMS materials has focused predominantly on verifying the function of an actual device under ideal circumstances (e.g., no surface contamination, clean, low-humidity environment) evaluating fatigue and wear of the system, rather than evaluating the intrinsic environmental resistance properties of the component materials. Little, if any, research has been conducted on evaluating the long-term EAC resistance of MEMS materials in realistic aggressive environments (of any severity). Furthermore, there has been no relevant work aimed at devising a means to assess the resistance of MEMS materials to EAC.

The research proposed here addresses this critical need by providing a new technique to assess the EAC resistance of MEMS materials. The information provided through this new technique will enable the establishment of appropriate combinations of environment (defining packaging requirements), local stress levels (device design), and metallurgical factors (composition, grain size and orientation) that must be achieved to prevent EAC in future MEMS applications.

Technical Issues

1. Existing knowledge base on EAC susceptibility of bulk materials can not be used to assess the behavior of the micro-scale materials within a MEMS device: Due to the large difference in size scale, microstructure, and material chemistry, literature data on the EAC of silicon and nickel alloys provides only a crude starting point for understanding the same degradation processes in MEMS materials. Additionally, the extent/magnitude (e.g., crack length) of acceptable attack that is relevant for a MEMS device is orders of magnitude less than that which would be considered significant, or in many cases, detectible, for a larger, structural bulk material. As an example, crack growth rates on the order of 10^{-12} m/s are important for these small-scale devices, whereas such rates would be considered negligible (either undetected or ignored as insignificant) for larger scale structures from which our current understanding of such phenomena is based. Furthermore, the literature has demonstrated that purely mechanical fracture processes for small-scale structures, such as those used in MEMS, differs largely from that observed on the bulk material. Thus, the direct application of existing literature/understanding of such materials is not possible.

2. The small size scale of MEMS materials prohibits application of conventional fracture mechanics techniques: The experimental procedures presently used to evaluate the EAC characteristics of a bulk material (i.e., sample geometry, environmental and mechanical control systems, etc.) simply cannot, without

extensive modification, be physically applied to the very small-scale MEMS samples, nor is their sensitivity adequate to detect damage on the scale that must be detected for a MEMS device. Novel sample configurations, test chamber/environmental control systems, mechanical loading, and measurement instrumentation must be developed such that these micro-scale MEMS materials can be reproducibly evaluated.

Technical Approach

The goal of the research proposed here is to develop an integrated environmental and mechanical technique that can be used to properly assess the susceptibility of MEMS materials to EAC. The resulting technology will include the means to precisely instrument selected sample designs, to control the mechanical stress state and environmental conditions during the test, and to effectively analyze the resulting data. The material set will consist of nickel-based LIGA specimens with well-defined chemical and mechanical characteristics. The initial approach can be broken down into three main tasks that collectively will define and validate the experimental technique.

Task 1: *Sample and Sensor Design*: Mechanical test specimens that can be readily characterized (in terms of the strength, ductility, and fracture characteristics of the material) will be fabricated. Once produced, each specimen will be instrumented with "electrical resistance" sensors produced via thin-film processing techniques. These sensors will provide much of the quantitative information required to identify and characterize the crack nucleation and growth process, as well as the general stress/strain state of the material throughout the test. An example of one such device is a thin-film crack length detection sensor that has been demonstrated in the literature for similar size scale specimens. Other sensors will include cutting-edge atmospheric corrosion sensors developed at Sandia (to understand the environmental conditions that exist, and electrochemical reactions that occur on the sample surface and approaching the crack tip), as well as electrodes that facilitate monitoring and/or controlling the electrochemical state of the system during the test. A significant complicating issue is that these sensors must themselves be electrochemically robust in the environments in which they are used. That is, they must not influence the fracture behavior of the materials being evaluated.

Task 2: *Mechanical, Electrical, and Electrochemical Instrumentation:* This task will consist of the selection and assembly of fixturing to mechanically stress, electrically and electrochemically monitor the specimens while simultaneously controlling the exposure environment. Both the samples and their associated sensors must be appropriately instrumented. Due to the size scale of the sensors as well as the phenomena being evaluated, the resultant signals will be very small. A system must be designed/specified that enables the appropriate currents and/or voltages to be accurately monitored, and then mathematically correlated to the phenomena which forms the basis of the signal.

Instrumentation previously assembled at Sandia to make extremely low current electrochemical measurements will be adapted to accomplish this. The second aspect of the test system is a means to mechanically stress the samples under relevant environmental conditions. As with the electrical instrumentation, the approach here will be to build upon systems previously developed and assembled at Sandia, modifying them to allow the addition of the instrumentation and permit the exposure of the test specimen to an experimentally relevant aqueous or atmospheric environment throughout the test.

Task 3: *Experimental Validation:* The final aspect of this work is the experimental validation of the technique. Initial validation experiments will be performed on a high sulfur, LIGA formed Ni – a material which, based upon our understanding of bulk alloys of similar composition, should be susceptible to EAC. This material will be evaluated throughout the development process, and compared to a low sulfur or other LIGA composition that should be less susceptible to EAC. Specimens with engineered defects simulating cracks or crack nuclei will be included in the test matrix. In addition, once refined, the technique will be applied to polysilicon specimens in environments believed to be both benign and aggressive based upon our understanding from the literature.

Initial Material System Selection

As the goal of this project is to develop a technique to evaluate the susceptibility of a material to EAC, it was essential that the material set selected for evaluation have a very high probability of undergoing EAC under a readily achievable set of experimental conditions. Watts nickel, a high sulfur, ultra fine grain electrodeposited nickel material (produced here through the LIGA process) was selected. Post fabrication thermal processing is utilized to alter the grain size and decorate the grain boundaries with a large concentration of sulfides, thereby producing a microstructure highly susceptible to EAC. More details on this material, including the microstructure resulting from the thermal processing, are given below.

The LIGA Process

The LIGA (Lithographie Galvannoformung, Abformung) process is utilized to produce microsystem components via electrodepositing metals through a pattered mold. The direct version of this process is show schematically in Figure 1.1 and is capable of producing discrete, free-standing metallic parts with lateral dimensions ranging from ~10 to ~1000 μm and thicknesses usually on the order of 100's of microns but potentially as thick as several millimeters. The process begins by exposing a wafer assembly, composed of a patterned X-ray lithography mask and a photoresist blank bonded to a conductive substrate, to X-ray synchrotron radiation. The typical photoresist is PMMA and the common substrate materials are metallized glass or a metallized silicon wafer. X-ray radiation renders the exposed portions of the PMMA susceptible to dissolution by an appropriate chemical developer permitting development

of a mold consisting of deep vertical cavity features with geometric tolerances on the order of 1 μm. The mold is then immersed in an electroplating bath and the cavities are filled with an electrodeposited metal or alloy. Subsequent processing steps involve planarization of the top surface, removal of the PMMA and chemical release of the final piece parts. For the present study, the LIGA process was used to fabricate to final shape, small tensile specimens and rectangular beams. An example of a typical pattern is shown in Figure 1.2 where a circularly symmetric pattern of tensile specimens is shown as deposited and still attached to the substrate.

The production of parts with thicknesses ranging from 100-2000 μm requires the mitigation of intrinsic stress build-up during deposition. High stresses can alter part dimensions and, in extreme cases, lead to mold fracture [Kelly 03]. Deposition stresses can be controlled by careful choice of processing conditions, bath additives, and deposit material. In this work, we investigated a deposit system where stress is reduced by the addition of sodium saccharin to a Watts bath electrolyte. The resulting deposit is characterized by a nanocrystalline microstructure and higher strength than conventional Ni electrodeposits due in part to the presence of sodium saccharin in the bath that refines the grain size [Nakamura 84, Natter 98, Jensen 03]. However, saccharin also contains sulfur that is adsorbed at the electrolyte-deposit interface and is therefore incorporated into the deposit at concentrations that can approach 1000 ppm depending on the saccharin concentration in the bath, deposition temperature and current density. This sulfur segregates to grain boundaries, leading to embrittlement at moderate temperatures [Lee 89, Klement 95, Hibbard 02, Jensen 03]. These deleterious effects, coupled with the onset of rapid, abnormal grain growth limits the usable temperature range for components produced with this bath composition.

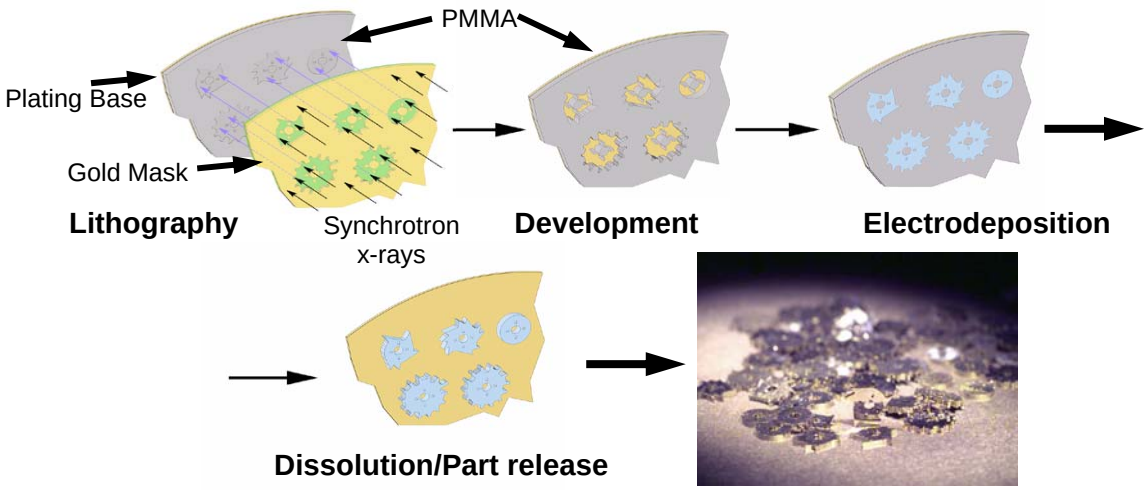

Figure 1.1: Schematic representation of the LIGA process

Figure 1.2: Tensile specimen mold

Section 2: FY04 Activities and Accomplishments

The goal of the first year of this project was to establish a mechanical test method, and demonstrate the feasibility of this approach for evaluating the environmental cracking susceptibility of MEMS materials, focusing first on high sulfur LIGA material. Once that is accomplished, a test system capable of performing multiple tests in a variety of environments will be constructed. In order to achieve this goal, 4 primary tasks must be completed. The results to date, and experimentation planned for the remainder of FY04 are detailed below.

Task 1: Mechanical Test System Development

The first challenge which had to be dealt with in this project was the selection and design of an appropriate test technique and associated apparatus to evaluate the mechanical properties of MEMS materials. Due to their small size, direct application of many traditional approaches was not possible, with one exception – bend testing. The three point bend test, as defined in ASTM C1421 and E399 was selected as the basis for the initial mechanical test system. A number of simplifications to the test technique itself had to be made due to the size scale of the materials being evaluated. The small size scale is necessary as the properties of bulk MEMS materials differ in many cases from actual MEMS parts. In other words, the wealth of existing data, or data which we might obtain, for the bulk form of these materials cannot be used to conclusively predict the performance of MEMS devices because the mechanical properties of our MEMS materials are, in general, very different than the bulk analogues.

The modifications to the standard test technique involved both the test apparatus as well as the sample geometry. In terms of the sample geometry, a valid 3-point bend test (in terms of assessing the mechanical properties of a material) requires a sample with a specific ratio of thickness and span – the sample is designed such that the ratio of the thickness to the width of the sample is between 1 and 4, with the span between the two loading points roughly equivalent to four times the thickness of the sample in the loading direction. As the sample gets very thin, this requires that the loading points also become very close together, and that they be very small in diameter. While this may certainly be possible later in the project as the test technique is refined, it is experimentally difficult to achieve for the proof of concept work being conducted at this stage of the project. In this case, the span between loading points is considerably larger than that required by the ASTM standards – as such, while the general nature of the stress state obtained in the sample will be known (i.e., highest tensile loading at the apex of the bend), the relationships defined for standard test samples will only provide an estimation of the actual stress state. For the test apparatus itself, the diameter and nature of the loading points was changed. In a standard test, two of the loading points are gimbaled, while one is fixed – in this case, all three are fixed. In addition, the ASTM standards require that the loading points be a small multiple of the thickness of the sample – in this case, a much larger diameter was used (again, for practical considerations). This will add an additional frictional component to the load, but while this will impact the accuracy of the expressions used to estimate the surface stress of

the sample, it will not reduce the validity of assessing the EAC susceptibility of the tested materials. The apparatus itself is illustrated in Figure 2.1. Several other aspects of the system worth noting are first that the loading points are ceramic, allowing the sample to be electrically isolated from the mechanical test apparatus (essential for the implementation of crack length detection or other electrochemical sensors). In addition, much of the load train (and all of the material which would be exposed to an aggressive environment) is made from stainless steel to prevent its degradation during testing. Finally, the system allows the position of the two outer loading points to be adjusted as dictated by the sample geometry in order to obtain the desired stress state on the surface of the sample. Sample loading is accomplished through the use of commercially available precision actuated stage and an appropriately sized load cell. This will allow both displacement and load based testing and monitoring.

Another aspect of the test system is environmental control – the ability to "dial in" specific combinations of aggressive species (e.g., H_2S, Cl_2, etc.), temperature, and humidity level. While this was initially planned to be accomplished in FY05, the decision was made to construct it ahead of schedule to simplify the assembly process of the overall test system (it was essential that the mechanical test apparatus be able to fit inside the environmental chamber, so they were built simultaneously). The system constructed was based upon other gas exposure systems in use within Dept. 1823, and utilizes permeation tubes (tubes which emit a contaminant at a known rate) combined with a complex flow control system to maintain a constant concentration of aggressive species as well as humidity level. The entire system is then placed within a temperature controlled chamber.

Task 2: Proof of Concept Testing

In FY04, proof of concept testing was conducted utilizing high-sulfur nickel formed through the LIGA process. Post production thermal processing was utilized to alter the grain size and grain boundary contaminant level to produce material with a range of EAC susceptibilities. Initial experiments focused on measuring the basic mechanical properties for the LIGA material, which was then compared to values obtained via other means. The LIGA material was rendered more susceptible to localized attack through thermal processing. Electrochemical data obtained using a micro-electrochemical cell has indicated that the microstructures which have been achieved through the aforementioned process have substantially increased electrochemical activity of the grain boundaries relative to the grain interiors. An example of the altered microstructure, and resulting local electrochemical activity, achieved through this treatment is illustrated in Figure 2.2. As a result of the increased activity of the grain boundaries relative to the grain interiors, we expect this material to be susceptible to classical intergranular EAC when exposed to an appropriate environment. EAC testing results confirmed this susceptibility.

Task 3: Development of Crack Detection Sensors

The crack length sensor currently under development consists of two gold pads, one located on either side of the location of maximum surface stress on the bend specimen (see Figure 2.3a below). These pads must be close enough to one another that they can effectively communicate (i.e., the surface resistance between the two pads must be less than that which can be dealt with by our instrumentation), as well as being electrically isolated from the sample and themselves. Several attempts were made to produce these sensors through the use of a spun coated SU-8 photoresist as the insulator, followed by deposition of the gold (using a shadow mask to prevent deposition on the region between the two pads). The resist was then developed and removed using either a wet or dry etching process. In the case of the dry etching process, significant damage to the sample resulted, as well as pinholing of the sensor pads, and shorting of the pads to the sample (and thus, to one another). The wet process was more successful, but still failed due to redeposition of gold on the edges of the sample, again shorting the gold pads to the sample surface, and thus to themselves.

The SU-8 approach has been abandoned. Presently, we are planning to use paralene as the resist (a more effective conformal coating). The gold will again be deposited using a shadow mask. The paralene will then be plasma etched from the surface, this time staggering the end of the resist and the gold pad as illustrated in Figure 2.3b.

Task 4: Sample Geometry/Processing Refinement

The initial sample geometry is, as indicated above, a rectangular section which has been cut from a larger plate of as-deposited material. As such, the initial proof of concept testing is being conducted on a material which can be considered to an extent as a bulk material. It does however retain a microstructure that is representative of that which would be found in formed-to-shape microsystem components. Nonetheless, the first step in sample refinement will be to electrodeposit net-shape samples which will be then be tested in the as-fabricated condition. The resulting surface structure (which will govern the crack initiation process) will be representative of an actual LIGA-MEMS part. In addition, the incorporation of formed-in-place defects (stress risers, such as a notch) into the as-formed sample is also being explored. To accomplish this, an effort is being made to have samples appropriately sized for this project incorporated into a mask used for actual LIGA parts.

FY05 Proposed Work

The goal of the work proposed for FY05 is essentially to refine the test technique defined in FY04, as well as expand its capabilities. This goal can be broken down into three specific (and interrelated) tasks:

Task 1: Crack Detection and Length Measurement

In FY04 the initial proof of concept work was completed for an initial crack detection sensor. Efforts in FY05 will focus on expanding the sensitivity of this technique in an effort to gain information on the crack growth process (i.e., obtaining the ability to identify the nature of a crack as it progresses, rather than just detecting initiation or an indication of when a crack has grown to a specific size. Accomplishing this task will require careful identification of the limitations of the current technique, then establishing and implementing appropriate improvements.

Task 2: Assessment of Atmospheric Corrosion Potential

In FY04, a gas exposure system was assembled which enabled precise control of the environmental conditions present within the test chamber. The implications of a particular environment, in terms of it's aggressiveness towards the sample material, must be understood. In this task, we will build upon previous efforts to create atmospheric corrosion sensors close to, or actually on, the test sample. Sensor construction will be similar in concept to others utilized within 1823, consisting of a layered construction of the sample material, an insulator, and a noble metal layer. These sensors will enable us to quantitatively assess the aggressiveness of the environment towards the sample material and provide a real-time, in-situ measurement of the electrochemical activity associated with crack advance.

Task 3: Sample Refinement

Initial experimentation has focused on bars of material which had been machined from a larger bulk material. While the composition of the material was similar to that of an actual component, the microstructure and physical properties may differ from a smaller, as plated part for reasons detailed previously. As such, in this task we will attempt to construct samples which are in the as plated condition – in other words, samples of a similar geometry to what has been used thus far, but which are plated as a single sample. We will also begin to explore the impact of induced defects in the sample surface, such as a notch, which may allow us to better control the crack initiation and propagation behavior.

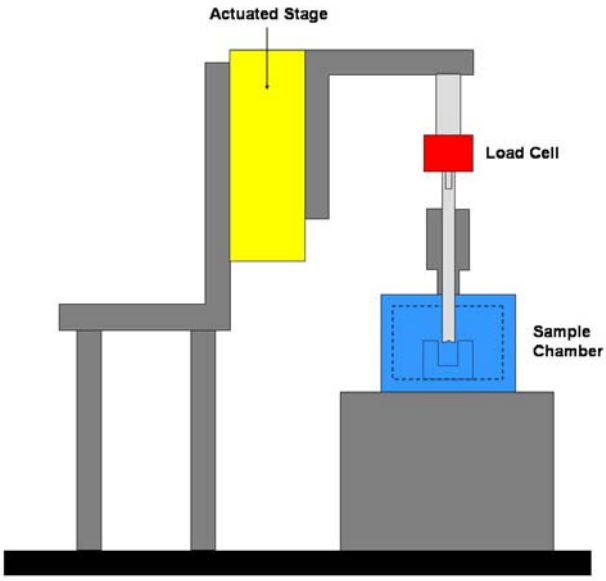

Figure 2.1: Modified 3-point bend mechanical test apparatus

a.

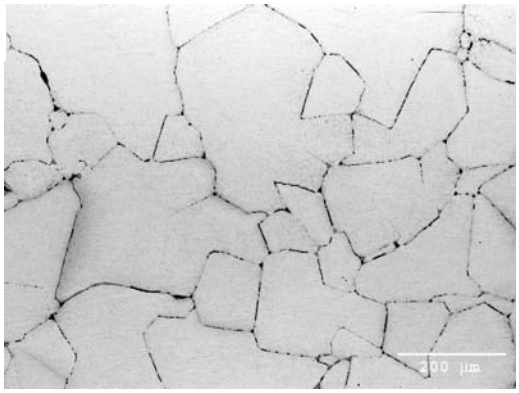

b.

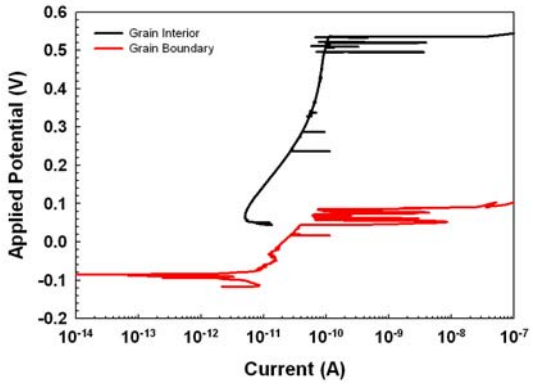

Figure 2.2: Impact of heat treatment (700^{o}C for 2 hours) on high-sulfur LIGA nickel. (a) microstructure (b) local electrochemical activity.

a

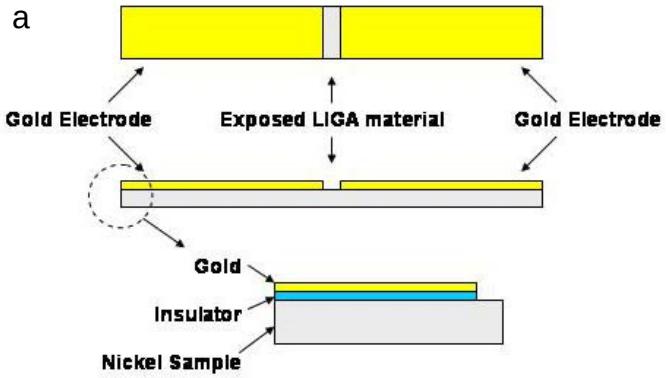

b.

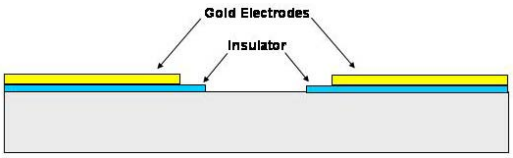

Figure 2.3: (a) Crack length detection sensor currently under development and planned alterations (b) to the leading edge of each gold pad.

Section 3: FY05 Activities and Accomplishments

The goal of the first year of this project was to establish a mechanical test method, and demonstrate the feasibility of this approach for evaluating the environmental cracking susceptibility of MEMS materials, focusing first on high sulfur LIGA material. While initial results were positive, it soon became clear that the initial test sample geometry and load application method was not able to provide the desired controlled crack initiation and propagation kinetics. The goal of the work performed during FY05 was essentially to refine the test technique developed in FY04, as well as expand its capabilities. The work conducted during the past FY can be broken down into three specific (and interrelated) tasks:

Task 1: Mechanical Test System and Crack Detection Sensor Development

The initial test method developed during FY04 was based loosely upon traditional 3-point bend tests as defined in the ASTM C1421 and E399 specifications. Unfortunately, while it was clear that environmental damage was occurring on the sample surface, this sample geometry was demonstrated to be incapable of causing environmentally assisted crack initiation. One this deficiency was clearly identified, efforts shifted to modifying the test technique such that crack initiation, and then propagation could be reproducibly achieved. The notched bend bar technique (Figure 3.1) was pursued as it would provide a better defined crack initiation point, as well as allow the application of a much higher stress intensity than the plain bend bar explored earlier in this project.

Development of the crack length detection sensor which was initiated in FY04 continued into FY05. The sensor itself was simple in design, consisting of two gold electrodes which were electrically isolated from the sample, and located on either side of the center of the bend bar (the most probable location of crack initiation). In FY04, several attempts were made to produce these sensors through the use of a spun coated SU-8 photoresist as the insulator, followed by deposition of the gold (using a shadow mask to prevent deposition on the region between the two pads), then patterning and developing of the resist. Several approaches were attempted for the latter two steps, but in both cases pin-hole formation in the insulator pads resulted, causing the sensors to be electrically shorted to the sample (and thus to one another). The SU-8 approach was then abandoned in favor of using paralene as the insulator (a more effective conformal coating). Once the paralene was deposited, the electrodes were produced in a similar manner as was used in the SU-8 case, save that the paralene was plasma etched from the surface. Unfortunately, despite our best efforts to prevent it, shorting of the sensors again resulted, and as such the development of the crack detection sensor was put on hold until a more promising insulator layer was identified.

As significant technical hurdles still exist to the development of an electrical or electrochemical based sensor to detect crack initiation, we believe that developing other techniques will give the project a higher probability of success. As such, an effort was made to identify other potential techniques which might be capable of observing the

environmental damage evolution, and a number of other surface sensitive techniques were identified which could potentially be applied to study microsystem materials. One in particular which has been targeted as being particularly promising is differential microscopy. In this technique, a series of high resolution images of the surface are taken over time and quantitatively compared to one another through image subtraction or some other similar post-processing method. Subtle changes in the surface morphology not readily resolvable using traditional image analysis techniques can then be readily quantified. One area in the literature where this is being developed is for the identification of pit nucleation on aluminum alloys. Here, the size scale and obscurity of the environmental attack being studied is similar to that which we are faced with on microsystems materials. In this particular application, the technique is proving to be capable of resolving subtle variations in surface morphology corresponding to pit nucleation which could not otherwise be seen. For this project, we will employ this technique to observe damage evolution on a MEMS part. While the immediate concern is to monitor crack nucleation from the sample surface, other types of damage such as pit nucleation, shear band formation, etc. should also be capable of being resolved. Electrochemical techniques offer the advantage of being able to 'see' into the crack; thus a combination of surface sensitive differential microscopy and electrochemical detection would provide the complete picture. However, a number of significant challenges must be overcome if such a technique is to be successfully developed for this application. First, image to image registry is critical – if the size scale of the features we are attempting to characterize is at the sub-micron level, then the images must be aligned in both the x and y directions at least that well. This becomes increasingly difficult as the magnification increases, or if multiple images must be taken to capture the region of interest then “stitched” together afterwards. In addition, a methodology for post processing of the images must be developed – this could be as simple as filtering the images such that certain features become more prominent and extraneous noise is removed, or it could be considerably more complex. At present, efforts are focused on developing a technique based upon differential microscopy that can be applied to our atmospheric exposure based environmentally assisted cracking studies.

Task 2: Assessment of Atmospheric Corrosion Susceptibility

In FY04, a gas exposure system was assembled which enabled precise control of the environmental conditions present within the test chamber. While this experimental setup allowed for defining the inlet concentration feeding the test chamber, the impact of consumption due to the chamber, sample, fixturing, etc. could not be readily accounted for. In order to address this concern, a chlorine detector capable of monitoring chlorine at the ppt level was identified, obtained and implemented. This new system enables precise control of the chlorine content within the chamber, and helps insure that experimental variability due to chamber consumption issues is minimized. Unfortunately, while this system is very sensitive to chlorine, it is also sensitive to NO_2, a major component in the mixed flowing gas systems commonly used to evaluate atmospheric corrosion of microsystem materials, hindering it’s effective use in future planned testing. However, a NO_2 to NO conversion system (NO does not interfere with

the Cl_2 signal) has been identified and will be implemented this FY which will prevent this interference, and allow proper application of the chlorine analyzer to the mixed flowing gas environments which we plan to apply in testing during FY06.

Task 3: Sample Refinement

Initial experimentation focused on bars of material which had been machined from a larger bulk material. While the composition of the material was similar to that of an actual component, the microstructure and physical properties may differ from a smaller, as plated part for reasons detailed previously. In FY05, samples were constructed from material in the as-plated state – in other words, materials were plated to the desired geometry, rather than being machined to it. As discussed above, the flat bend bar samples were incapable of generating the mechanical damage (i.e., EAC) which we desired. As such, samples with induced defects – in this case a blunt notch (see Figure 3.1) with a root radius of approximately 0.2mm - were machined using a fine diamond saw. This new sample geometry (and associated modified mechanical test system) provides a number of key features – first, a much larger and better defined stress intensity can be reproducibly applied to the material in a well defined region (i.e., the notch root). Second, the new geometry provides a "defect" more in line with the types of things we would be concerned with for an actual MEMS part, and finally, it provides a large portion of material through which a crack might propagate, improving our chances of having a stable crack which we could focus on for sensor development.

Experiments performed utilizing the new sample geometry have successfully illustrated that EAC of the high sulfur nickel can occur. A load vs. time plot for one such notched bend bar evaluated in a 50ppb Cl_2 atmosphere is presented in Figure 3.2. As shown in the figure, after an induction period of nearly 27 hours, the sample rapidly failed. The nature of the failure suggests several things. First, it clearly established that environmental effects can indeed result in the cracking of the Watts nickel – something the previous sample geometry was unable to demonstrate. Second, due to the rapid growth rate observed, the cracking process is largely initiation controlled. The latter point is likely the result of the sample geometry itself – once a crack has initiated, the applied stress intensity at the advancing crack tip is considerably higher than that which was applied at the notch root – as such, the crack is able to advance rapidly through the sample because the stress intensity does not fall off sufficiently with crack advance (and sample unloading) to arrest the crack. To test this hypothesis, the evaluation of samples with a notch/artificial defect with dimensions (i.e., root radius and aspect ratio) approaching that of a crack is planned for later this FY.

In the remainder of the FY, more effort will be focused on replicating this result, followed by careful SEM evaluation of the surface. This will provide two critical pieces of information – first, it will allow us to identify the nature of the defect which led to crack initiation, and second, it will help further our understanding of the mechanical behavior of this material. This new understanding of the crack initiation site will be used as input for the differential microscopy approach, providing valuable information on the type of

surface damage is important for the cracking process (i.e., identifying what to look for, and perhaps equally as important, what to ignore).

FY06 Proposed Work

The goal of the work proposed for FY06 is essentially to further refine the test technique defined thus far in the project, as well as expand its capabilities. This goal can be broken down into three specific tasks:

Task 1: Sample Refinement

In FY05, the samples used to evaluate the LIGA material progressed from specimens machined from a larger piece of material to as deposited bend bars. These bend bars were initially evaluated in the as-deposited condition, then later with a blunt notch which was machined into them using a diamond saw. The latter geometry was then successfully used to demonstrate EAC in Watts nickel. Unfortunately, this sample has several limitations – foremost among which is the difficulty in reproducing a sample with a known notch depth and uniform notch root radius. In FY06 we will address this issue by producing samples which have the desired defect (i.e., notch) present in the as plated condition. This will enable the production of a series of well defined, and highly reproducible samples, which should provide better control over the crack initiation and propagation behavior.

Task 2: Assessment of Atmospheric Corrosion Susceptibility

Differential imaging microscopy has been identified as a particularly promising technique for quantifying the crack initiation process, as well as characterizing the environmental damage (e.g., pitting) which leads up to crack initiation. In FY06, considerable effort will be expended on applying this technique to the mechanical test samples discussed above. The imaging system, modified test chamber, and image post-processing methodology will be developed.

Task 3: Crack Detection and Length Measurement

In FY05, it was established that the Watts nickel material is indeed subject to environmentally assisted cracking, and conditions which cause that behavior were identified. In FY06, efforts will continue to define the window in which this material is susceptible to EAC, while subsequently working to develop a sensor to detect crack initiation. As efforts using SU-8 and Paralene have failed to result in a viable sensor, an attempt will be made to deposit an electrophoretic coating. This coating has been successfully applied in the past to produce similar layered sensors, and as such it is anticipated that it will work here as well. This new sensor will be combined with the differential imaging technique (described below) to form a system which is capable of resolving not only the crack initiation process, but also the damage process leading up to crack initiation.

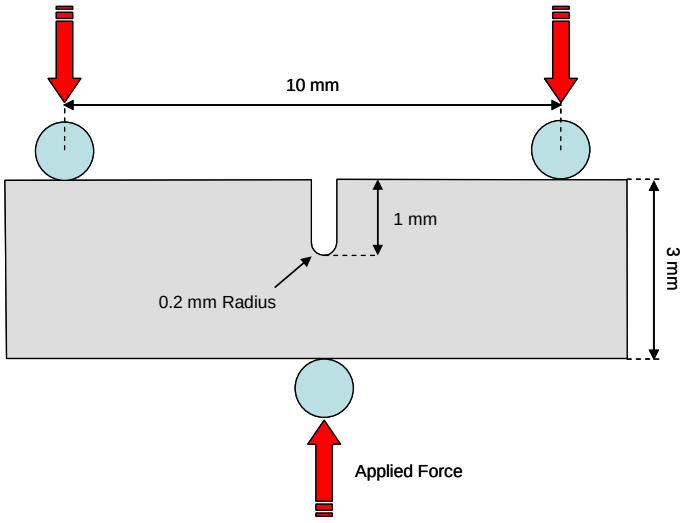

Figure 3.1: Notched bend bar geometry and loading points.

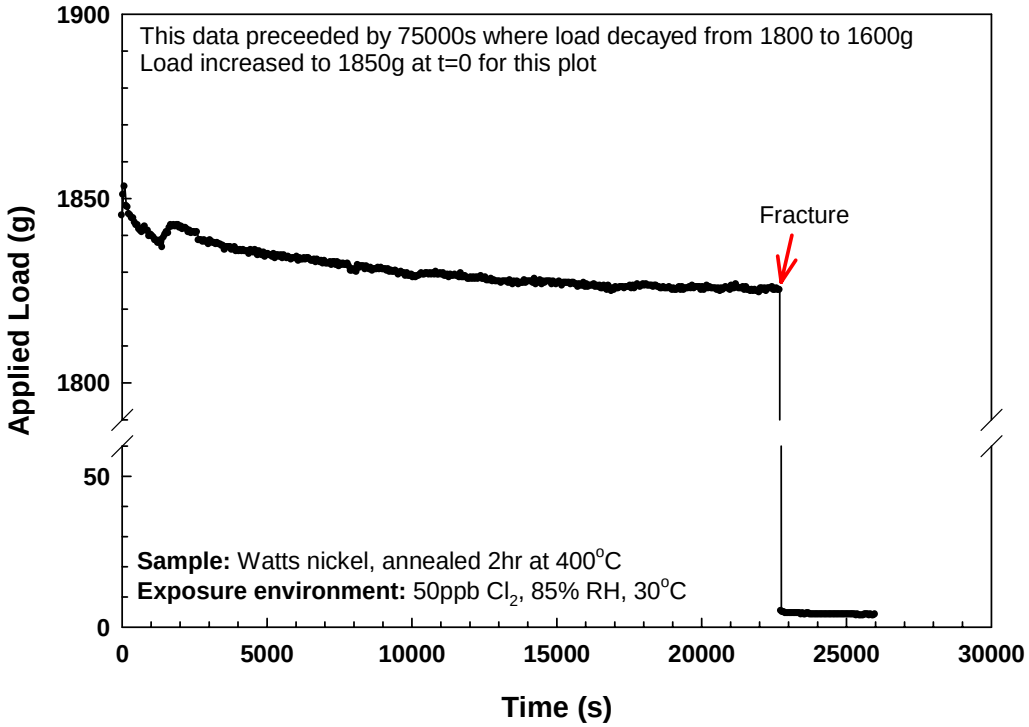

Figure 3.2: Load vs. time plot for a notched bend bar of the geometry pictured in Figure 1 which failed due to environmentally assisted cracking.

Section 4: FY06 Accomplishments, Program Summary, and Recommendations for Future Work

The goal of the work proposed for FY06 was to further refine the test technique defined thus far in the project, as well as expand its capabilities. This goal can be broken down into three specific tasks:

Task 1: Sample Refinement

As discussed above, one of the limitations which we were faced with in FY04 and FY05 was the lack of as-plated samples. As a result, geometrically important features, such as the notch, had to be machined into the specimen (in this case, cut with a narrow diamond saw). Due to the size scale of the samples, and the inherent surface roughness resulting from the machining process, samples produced in this manner were microscopically non-uniform at the notch root, and exhibited inconsistent mechanical behavior.

In order to address the non-uniformities discussed above, it was critical that samples with whatever stress enhancing features were desired be produced in the as-plated condition. Samples produced in this manner would have nominally identical notch geometries, eliminate non-uniformities in the notch root due to the production process used for past samples, and more uniform compositional and mechanical properties for samples taken from the same wafer. As such, a mask for new samples was completed, and several wafers of parts produced. A schematic of the wafer itself is shown in Figure 4.1, followed by an image of one of the notches produced in Figure 4.2, illustrating the uniformity of the notch root. Each wafer contained samples with four increasingly acute notch geometries. Actual radii were 0.25mm, 0.1 mm, 0.05 mm, and a “sharp” notch which was essentially a 0.05 mm wide “V” with a notch root radius of 0.005 mm.

Net-shape, though mold-structures were prepared via the LIGA method (as outlined in Section 1) using a Watts bath chemistry with the composition and process conditions as listed in Table 4.1. The addition of saccharin to the electrolyte resulted in the incorporation of approximately 700 ppm (wt.%) sulfur in the deposit.

Table 4.1: Bath Composition and Operating Conditions

Ni sulfate hexahydrate ($NiSO_4 \cdot 6H_2O$)	240 g/L
Ni chloride hexahydrate ($NiCl_2 \cdot 6H_2O$)	40 g/L
Boric acid (H_3BO_3)	30 g/L
Sodium saccharin ($C_7H_4NO_3S)Na$	1 g/L
SDS	0.2 g/L
Temperature	33ºC
pH	3
Current density	15 mA cm^{-2}

Room temperature tensile strength and ductility of the electrodeposit were directly measured using an Instron (Canton, MA) Model 5848 Microtester mechanical test frame and a non-contacting EIR laser extensometer. The specimens were fabricated with a gage length of 3.08 mm, a gage width of 0.76 mm and were between 0.2 and 0.3 mm thick.

As-plated Watts nickel is characterized as a high strength electrodeposit with good ductility. Figure 4.3a shows a family of tensile curves for the material. In the as-plated condition the, deposit exhibits a yield strength of approximately 1200 MPa, a UTS of 1800 MPa and greater than 10% strain to failure. Annealing induces a profound loss in ductility the onset of which is evident at temperatures as low as 100°C. With increasing temperature, the residual ductility continues to decrease, until at 300°C the ductility is nil (Figure 4.4). At this and higher temperatures, specimens fail during their initial elastic loading with virtual no permanent plastic deformation. This is illustrated more clearly in the inset in Figure 4.3 that shows the tensile curve for a specimen annealed at 500°C. The actual measured plastic strain is only approximately 0.02%. Fracture in these embrittled specimens is entirely intergranular. And an example of this is shown in Figure 4.3b.

Work on similar sulfur-bearing nickel electrodeposits has shown unambiguously that S partitions to grain boundaries during annealing at the temperatures shown here. Figure 4.5 shows an example of this sulfur partitioning in a Ni-Fe electrodeposit, containing similar amounts of S (Buchheit, et al.). The intergranular nature of the fracture is evident in Figure 4.5a and the associated sputter Auger traces in Figure 4.5b reveal a grain boundary facet concentration of sulfur that exceeds 10 at.%, falling to negligible levels after very short sputtering times.

Task 2: Assessment of Atmospheric Corrosion Susceptibility

In FY05, a condition was identified under which Watts nickel was susceptible to atmospherically induced environmentally assisted cracking. In FY06, experiments were conducted to explore this phenomenon more completely, attempting to identify if there was a threshold condition associated with crack initiation. In order to simplify things, the only variable was relative humidity (the temperature remained fixed at 30°C, and the chlorine concentration at 50 ppb).

As illustrated above, the yield strength and ultimate tensile strength for annealed Watts nickel is a strong function of the annealing temperature. Samples were vacuum annealed for two hours at 400°C prior to conducting each experiment. The applied load was selected such that the maximum stress in front of the notch was approximately 80% of the yield strength of the material. Stress concentration calculations were conducted using the relationship derived for a thin element with a notch on one side loaded in bending by Leven and Frocht (1953).

Table 4.2 presents the time to failure for samples exposed to the above conditions at various relative humidity levels. Additional experiments performed on

unannealed samples at 85% RH resulted in no failures after a period of one month (at which point the experiments were ceased). As can be seen in the table, there appears to be a threshold relative humidity between 50 and 60% RH below which crack initiation will not occur.

Table 4.2: Time to failure for notched tensile bars at 30°C and 50 ppb Cl_2

RH	250 µm	100 µm	50 µm	5 µm
85	2 days	--	--	--
65	5 days	2 days	1 day	1 day
60	4 days	6 days, 3 days	3 days	4 days
50	*No Failure*	*No Failure*	*No Failure*	*No Failure*

Fracture was intergranular in nature, and there was no visible transition from a stress corrosion crack to tensile overload on the fracture surface. Similarly, the load and crosshead displacement vs. time plots always transitioned rapidly (typically on the order of seconds) from fully loaded to failed – no evidence of slow crack propagation was observed. Based upon the mechanical properties of the aged material, specifically the near complete lack of ductility, the fact that failure was largely nucleation controlled was to be expected. (i.e., due to the low ductility, and hence low fracture toughness, crack blunting would be minimal, and as such, a crack, once initiated, would advance through the sample) Looking at the leading edge of the fracture surfaces, there were one or more large pit sites (Figure 4.6) for all samples. These large pits would be potent stress concentrators, and were likely the site of crack initiation.

Figure 4.7 illustrates the surface morphology of the samples following exposure to each environment. As the relative humidity was increased, the number density of pit sites also increased. In addition, at a RH of 60%, a population of larger, deep pits begins to form. As the RH continued to increase, these larger pits increase in aspect ratio (i.e., they start to become smaller in diameter, but extend deeper into the material.). At 85% RH, the large pits have become much higher in density, and very high in aspect ratio. While clearly much work is still needed to more thoroughly evaluate the crack initiation process, looking at the mechanical testing data available to date, a reasonable conclusion would be that these larger, high-aspect ratio pits act as stress raisers which then result in crack initiation. As the relative humidity increases, the acuity of these pits, which act as secondary notches in a way, increases, which may explain the reduction in time to failure with increasing RH. The lack of crack initiation at an RH of 50% and below is consistent with this in that no large, high aspect ratio pits were observed on the metal surface following as much as a month of exposure.

Task 3: Crack Detection and Length Measurement

One of the challenges which this program has attempted to overcome is the development of a crack initiation and propagation detection system. Efforts initially in FY04 and FY05 focused on developing a sensor on the test sample itself. Unfortunately, these attempts did not meet with much success. As a result, an

alternative approach was pursued in FY06. Development began on a technique based upon differential imaging microscopy which allows the researcher to deconvolute optically complex images (due to surface morphology, etc.), extracting only the degradation response (represented as changes in the image). This would allow complex sample geometries, as are present on MEMS devices, to be evaluated as the system functioned, without introducing potential defects/failure sources due to a sensor added to the device itself. Due to the large optical train which was required (camera, lenses, coaxial light source, etc.), the differential imaging system could not readily be adapted onto the mechanical test system. This isn't to say it couldn't be done, just that due to the time remaining on the project, it was not feasible. As such, an alternative material system was utilized for initial proof of concept testing. The atmospheric sulfidation of connector materials such as gold plated copper lend themselves to this technique, as the corrosion sites which are monitored for such materials are often difficult to observe due to the surface morphology of the plated copper. As mentioned above, an imaging system consisting of a camera, optical train, and mechanical translation stages was assembled. Proof of concept experiments demonstrated that this technique is capable of monitoring subtle changes in the surface, in this case the initiation of pore corrosion, previously unresolved experimentally. Figure 4.8 presents two images separated by approximately one day – individually, it is easy to miss the small differences in the second image due to corrosion product production at a single site on the surface. By using image subtraction, however, this site becomes readily visible. There are, however, a number of experimental difficulties which must still be overcome. These include image registration (as a shift of a single pixel can result in the observation of "differences" which aren't really there. A similar issue can occur with variations in lighting which may occur over time (though the use of a solid state lighting source does alleviate this to a degree). Future work will focus on addressing these discrepancies through a combination of mechanical and software based approaches.

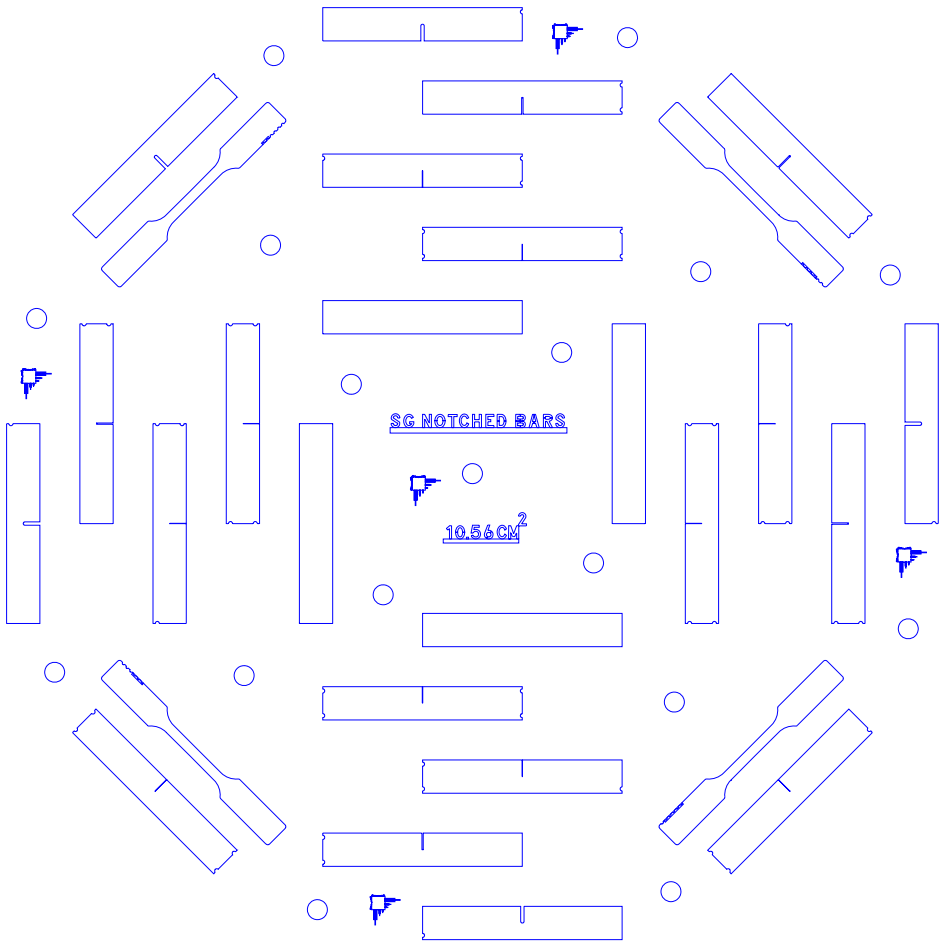

Figure 4.1: Wafer design used to produce notched tensile bars used in this study.

Figure 4.2: Optical microscopy of uniform notch root typical of the as-plated tensile bars.

a.

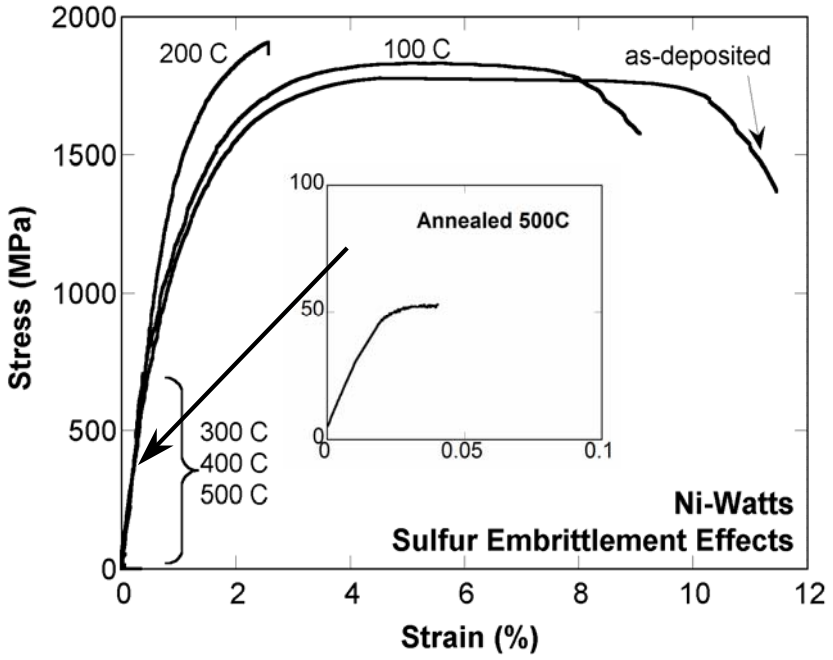

b.

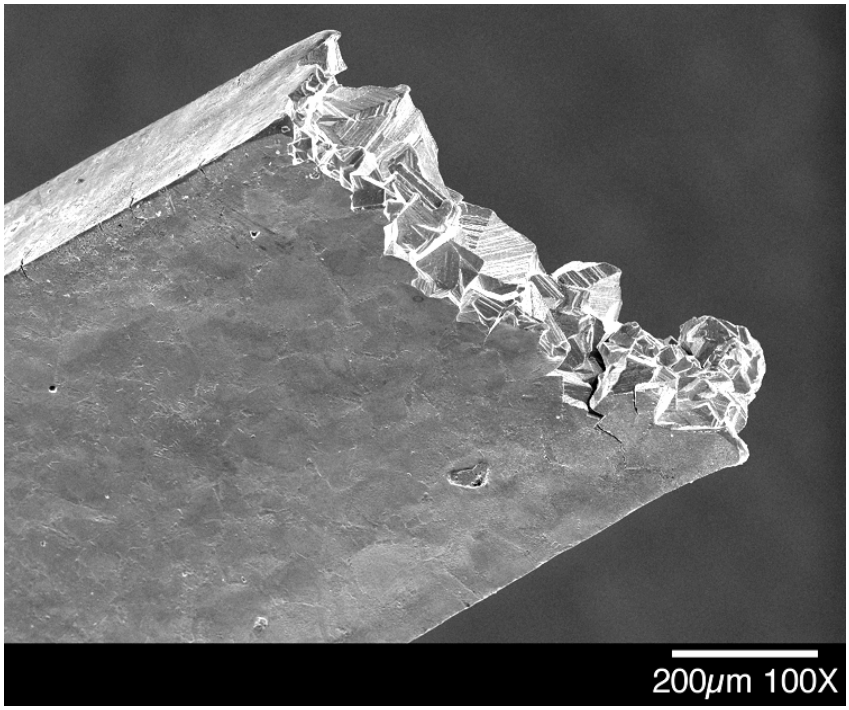

Figure 4.3: (a) Stress strain curves typical of Watts nickel prior to and following annealing at several temperatures. Note the large reduction in ultimate tensile strength and ductility illustrated in the inset graph. (b) Fracture surface of an annealed sample, illustrating the intergranular nature of the fracture.

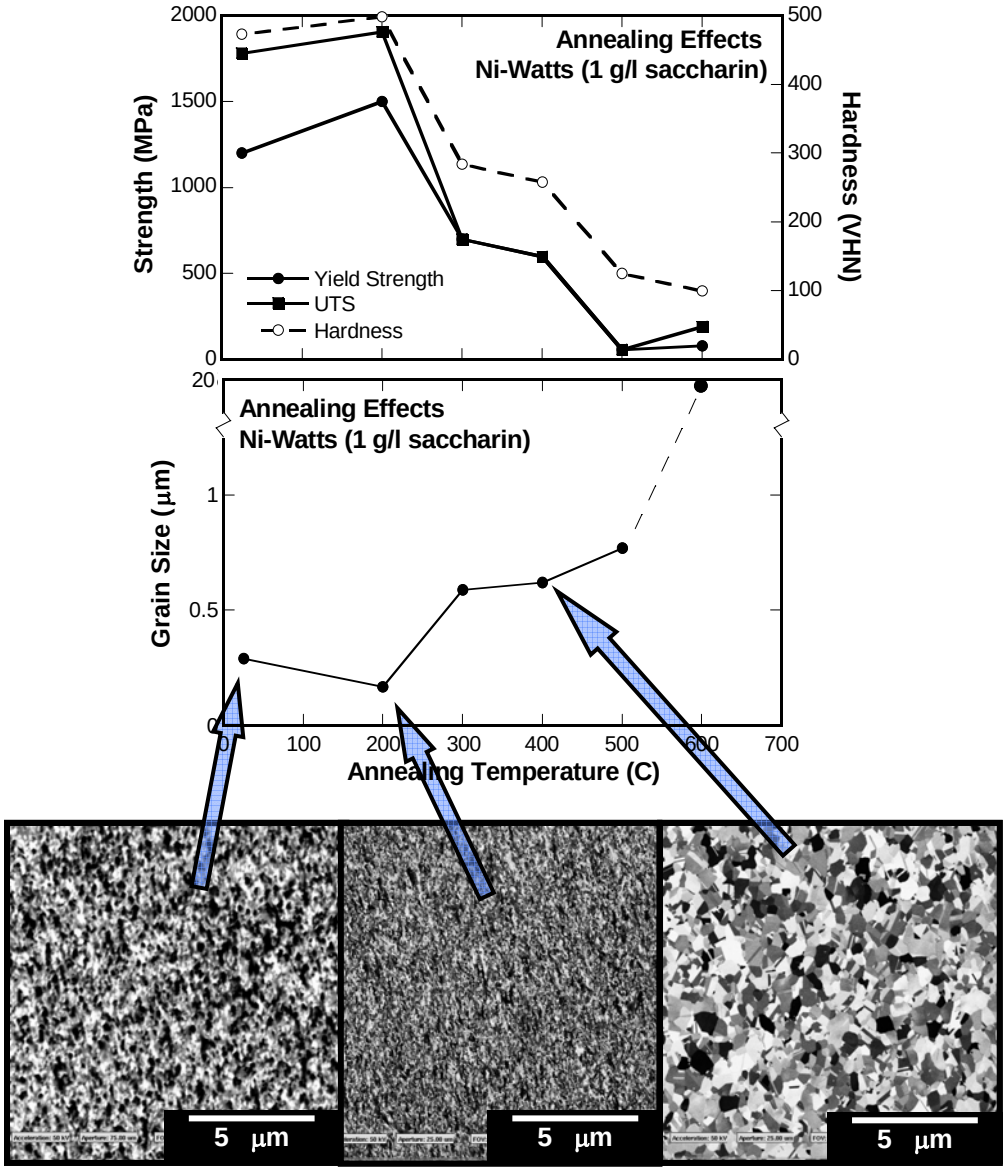

Figure 4.4: Impact of annealing on the mechanical properties and microstructure of LIGA formed Watt's nickel.

a.

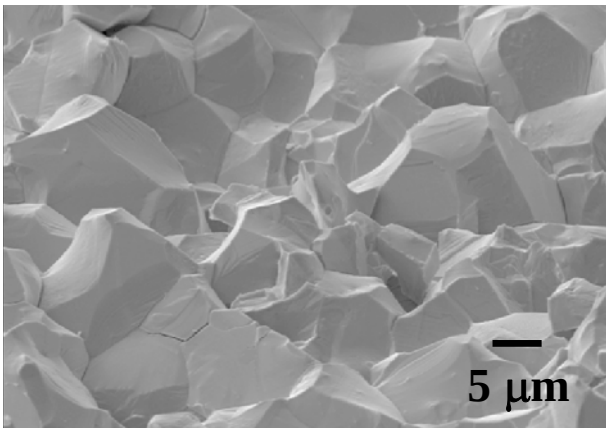

b.

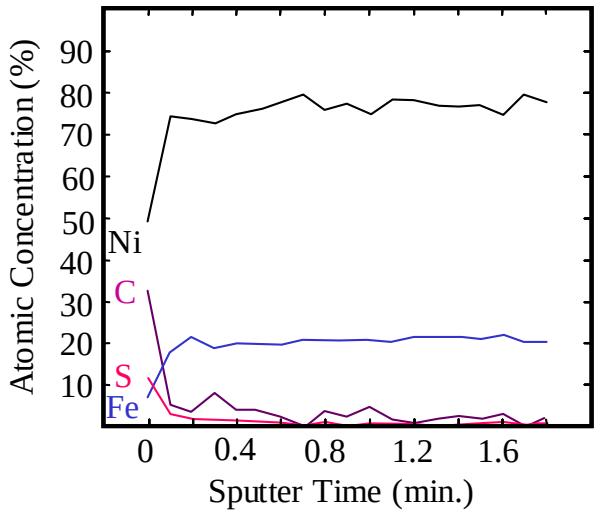

Figure 4.5: (a) SEM image of fracture surface from a tested LIGA Ni-Fe tensile coupon that was annealed at 700ºC for 1 hour. (b) Auger sputter depth profile from a location on the fracture surface. Sputter rate was approximately 5 nm per minute.

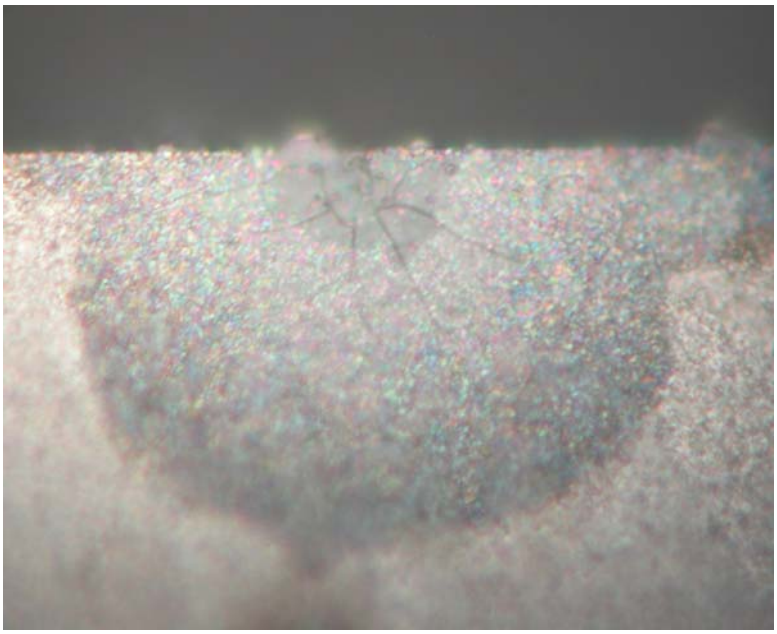

Figure 4.6: Typical image of the leading edge of a fracture surface. Shown here is a large pit and associated corrosion product for a sample exposed to 85% RH, 50 ppb Cl_2, at a temperature of 30°C. A number of such pits were observed on all failed samples, always at the leading edge of the fracture surface, as shown here.

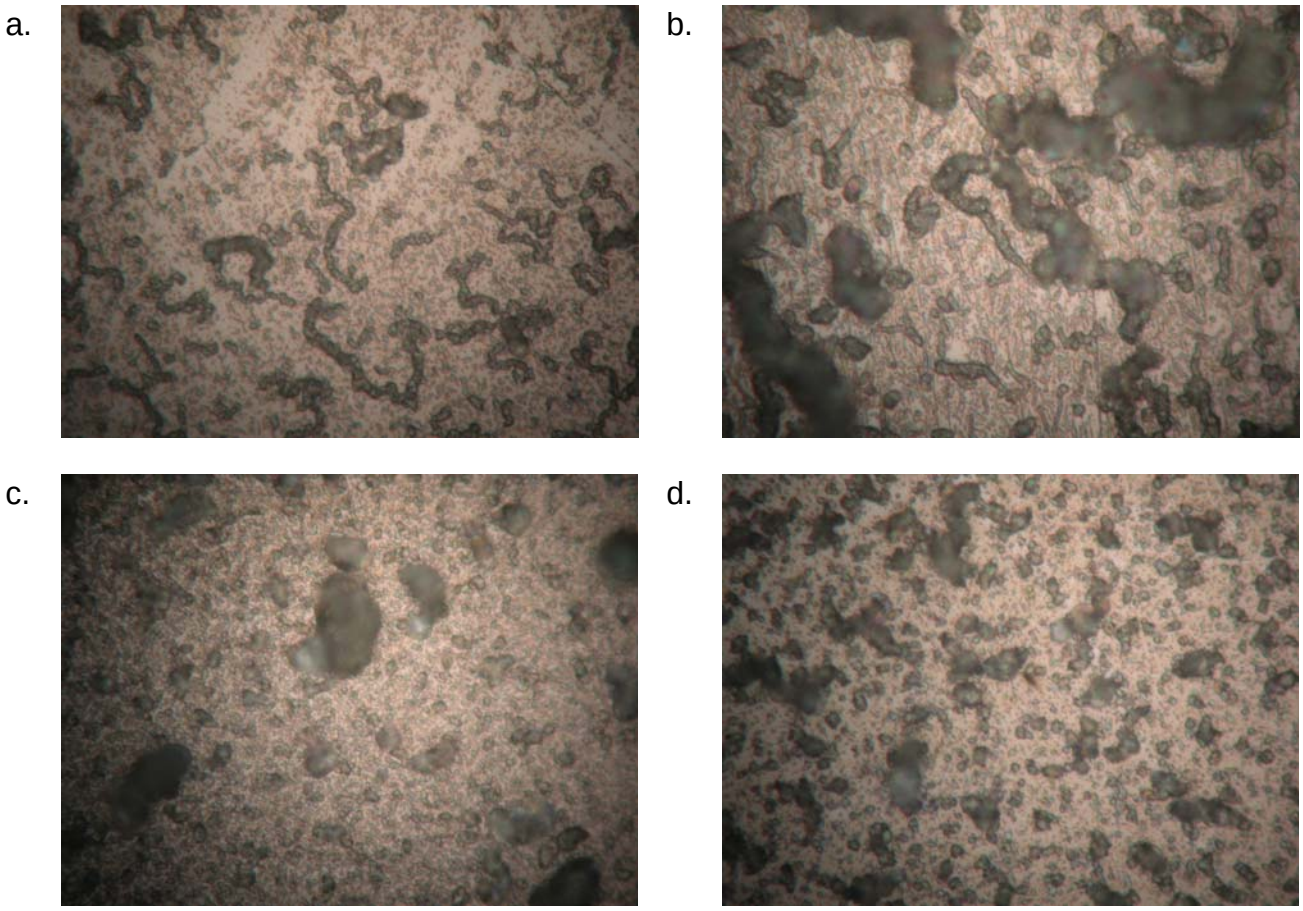

Figure 4.7: Optical microscopy (1000x) of surface morphology following exposure to 50ppb Cl_2, 30°C, at 50%RH (a), 60%RH (b), 65% RH (c), and 85% RH (d). As the relative humidity increased, the number density of pit sites increased, then at 60% RH a population of large pits began to form. The number and depth of these pits also increased as the relative humidity increased.

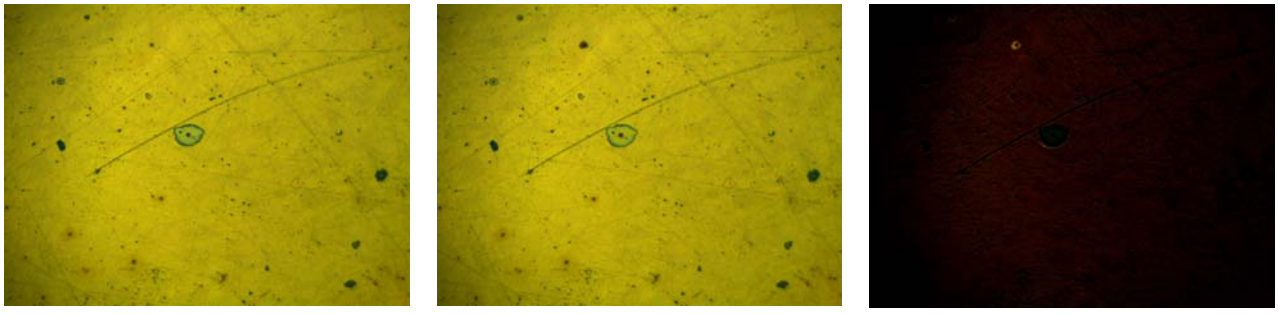

Figure 4.8: The first two images represent views of the same region on a gold plated copper surface undergoing sulfidation. The third image illustrates how image subtraction allows the regions which have changed (in this case due to the formation of copper sulfide corrosion product) to be clearly observed.

Program Summary

The goal of this program was to develop an integrated environmental and mechanical technique that could be used to properly assess the susceptibility of MEMS materials to EAC. A number of areas were explored in an effort to meet that goal:

1. A mechanical test system and associated control software was constructed, along with a means to accurately control the exposure environment (i.e., T, %RH, and contaminant level).

2. A material was identified which was susceptible to atmospherically induced environmentally assisted cracking. A threshold relative humidity was identified for a fixed contaminant level. Based upon the results to date, crack initiation appears to occur at large pits located, in this case, at the base of the notched for a notched bar loaded in bending.

3. An attempt to form surface mounted sensors capable of detecting crack initiation and advance was made – however, none of the geometries explored were successful

4. Proof of concept work was completed for a differential imaging system. The resulting technique is highly sensitive to changes on the surface optically complex systems. As such, this technique could readily be applied to observe the behavior of nearly any device, allowing for direct observation of a MEMS device, as an example.

Future Direction

If this work is to be continued, there are a number of key areas which need to be investigated in more detail, as listed below.

1. Experimental test system improvements – the existing test fixture evolved as the project progressed – as such, it became increasingly non-ideal with time. Some of the areas which should be addressed are the need for a more user friendly loading procedure, the addition of a semi-articulated test fixture as illustrated in ASTM C1421, and an improved bellows system to provide the dynamic seal over the mechanical test system.

2. Implementation of the differential imaging technique – the differential imaging system requires considerable space for the optical train, as well as an optically true window to view the sample during an experiment. The current system did not have sufficient space to incorporate this, but a redesigned chamber could.

3. Much more work is needed to better describe the atmospherically induced environmentally assisted cracking of Watt's nickel. In particular, identification

of the key features which dictate corrosion initiation (e.g., pit geometry, pit nucleation rate and growth behavior, etc.)

References

Kelly JJ, Goods SH, Yang NYC. Electro Solid State Lett 2003;C88:6.

Nakamura K and Hayashi T. Metal Finishing 1984;82:49.

Natter H, Schmelzer M, and Hempelmann R. J Mater Res 1998;13:1186.

Jensen JAD, Persson POA, Pantleon J, Oden M, Hultman L, and Somers MAJ. Surf Coat Technol 2003;172:79.

Lee TC, Robertson IM, Birnbaum HK. Acta Metall 1989;37:407.

Klement U, Erb U, El-Sherik AM, and Aust KT. Mat Sci Engr A 1995;203:177.

Hibbard GD, McCrea JL, Palumbo G, Aust KT, and Erb U. Scripta Mater. 2002;47:83.

Buchheit TE, Goods, SH, Kotula, Hvala,

Distribution

# Copies	Mail Stop	Name	Org
1	0888	David Enos	1823
1	9403	Steven Goods	8758
1	0888	Lysle Serna	1823
1	0888	Doug Wall	1823
2	9018	Central Technical Files	8944-2
2	0899	Technical Library	4536


Sandia National Laboratories